

Reversible Lattice Repacking Illustrates the Temperature Dependence of Macromolecular Interactions

Douglas H. Juers and Brian W. Matthews*

*Institute of Molecular Biology
Howard Hughes Medical
Institute and Department of
Physics, 1229 University of
Oregon, Eugene, OR 97403-
1229, USA*

Flash-freezing, which has become routine in macromolecular X-ray crystallography, causes the crystal to contract substantially. In the case of *Escherichia coli* β -galactosidase the changes are reversible and are shown to be due to lattice repacking. On cooling, the area of the protein surface involved in lattice contacts increases by 50%. There are substantial alterations in intermolecular contacts, these changes being dominated by the long, polar side-chains. For entropic reasons such side-chains, as well as surface solvent molecules, tend to be somewhat disordered at room temperature but can form extensive hydrogen-bonded networks on cooling. Low-temperature density measurements suggest that, at least in some cases, the beneficial effect of cryosolvents may be due to a density increase on vitrification which reduces the volume of bulk solvent that needs to be expelled from the crystal. Analysis of β -galactosidase and several other proteins suggests that both intramolecular and intermolecular contact interfaces can be perturbed by cryocooling but that the changes tend to be more dramatic in the latter case. The temperature-dependence of the intermolecular interactions suggests that caution may be necessary in interpreting protein-protein and protein-nucleic acid interactions based on low-temperature crystal structures.

© 2001 Academic Press

Keywords: cryo-cooling; contraction; vitrification; macromolecular interactions; β -galactosidase

*Corresponding author

Introduction

Crystals of a simple salt and of a complicated macromolecule are both defined by an ordered lattice which scatters X-rays according to Bragg's Law. The obvious difference is one of scale, where the repeating unit (the unit cell) consists of only two atoms for sodium chloride but several thousands in the case of macromolecular crystals. In terms of lattice packing, this difference has several consequences. First, the interstices in a sodium chloride crystal are too small to accommodate any other atoms, while in a macromolecular crystal they can be quite large and are filled with disordered solvent molecules (bulk solvent). Second, in a sodium chloride crystal all of the atoms are involved in lattice contacts, which tends to enforce order. In contrast, only a small fraction of the atoms are involved in lattice contacts in a macromolecular crystal, causing the crystal to be more

flexible. The other atoms are either buried inside the macromolecule, or are exposed on the surface and bathed by the disordered solvent. Often the surface residues are themselves disordered.

Macromolecular crystals are typically grown at 4–20 °C, but, in order to reduce radiation damage, the X-ray scattering data are often measured at cryogenic temperature (~100 K).^{1,2} This is especially true at synchrotron radiation sources where a crystal may only last a few seconds in the X-ray beam at room temperature. This means that the structure is determined at a temperature much lower than that at which the macromolecule is biologically active. In a typical experiment the crystal is first equilibrated with a cryoprotectant solution and then flash-cooled in a stream of nitrogen vapor prior to data collection. The cooling process takes ~0.1–1.0 second³ and usually vitrifies the bulk solvent. A common result of cryocooling macromolecular crystals is a unit cell contraction of 2–7% (Table 1),^{4–18} whereas sodium chloride contracts by about 2% over the same temperature range.¹⁹ The temperature-dependence of protein

E-mail address of the corresponding author:
brian@uoxray.uoregon.edu

Table 1. Contraction of crystalline proteins and their unit cells on cooling

Protein	ΔT (K)	α_{cell} (10^{-6} K^{-1})	α_{prot} (10^{-6} K^{-1})	$\alpha_{\text{cell}}/\alpha_{\text{prot}}$	Δ_{cell} (%)	Δ_{prot} (%)	Reference
Plastocyanin	122	118 (156)	59 (78)	2.0	-4.2	-1.4	4
RNase A	222	58 (117)	30 (61)	1.9	-3.8	-1.0	5
HEWL	200	128 (277)	37 (80)	3.5	-7.4	-2.1	6
HEWL	198	80 (167)	54 (113)	1.5	-4.6	-1.9	7
HEWL	198	59 (123)	48 (100)	1.2	-3.4	-1.0	8
HEWL	198	59 (123)	10 (21)	5.9	-3.4	-0.7	8
Flavodoxin	172	105 (195)	58 (108)	1.8	-5.3	-2.4	9
IL1 β	195	70 (147)	26 (54)	4.5	-4.0	-1.8	
Metmyoglobin	200	90 (206)	50 (115)	1.8	-5.2	-3.0	10,11
T4L	195	71 (148)	41 (86)	1.7	-4.0	-0.7	
α -Lytic protease	178	42 (80)	13 (24)	3.3	-2.2	-0.7	12
γ B-crystallin	143	112 (176)	39 (61)	2.9	-4.7	-0.3	13
Trypsinogen	192	1 (2)	-1 (-2)	--	0.0	-2.3	14
β -Trypsin (L-form)	193	65 (137)	26 (55)	2.5	-3.7	-1.5	15
Trypsin	175	58 (110)	17 (32)	3.4	-3.0	+0.1	16
β -Lactamase	175	89 (168)	32 (60)	2.8	-4.6	-2.2	17
10T	193	95 (201)	10 (21)	9.5	-5.4	-0.6	18
cS82R	193	85 (180)	13 (28)	6.5	-4.8	-0.8	18
β -Galactosidase	195	90 (190)	27 (57)	3.3	-5.2	-1.0	
Average	186	78 (153)	31 (61)	3.2	-4.2	-1.3	

The proteins in the Table are listed in increasing molecular mass (see Table 2). ΔT is the reduction in temperature, α_{cell} and α_{prot} are the linear thermal expansion coefficients of the unit cell and the protein, respectively. Δ_{cell} and Δ_{prot} are the fractional changes in the unit cell and the protein volumes. HEWL is hen egg-white lysozyme, 10T and cS82R are variants of 3-isopropylmalate dehydrogenase, T4L is bacteriophage T4 lysozyme (unpublished results of Blaine Mooers & B.W.M.), IL1 β is interleukin 1 β (unpublished results of Michael Quillin and B.W.M.). To our knowledge the Table includes all cases where both the refined low and high-temperature crystal structures have been reported and includes examples with and without cryoprotectant. In all cases, the crystal was flash-cooled, except for trypsinogen, which was cooled over several minutes. α_{cell} is the average taken over the three unit cell axes (e.g. for the a cell edge $\alpha_{\text{cell}} = \Delta a/a\Delta T$; for the monoclinic cells, a , $\sin\beta$, b and c were used). α_{prot} is obtained by averaging all center-of-mass to atom distances in the protein.¹¹ The values in parentheses are corrected to room temperature, to allow for an expected linear dependence of α with temperature between the glass transition temperature, T_g (assumed to be 180 K), and room temperature. Any temperature-dependence of α below T_g is not accounted for (see ref. 11). The change in the volume of the protein, Δ_{prot} is obtained using the method of Connolly⁴⁸ in which a spherical probe ($r = 1.4 \text{ \AA}$) is rolled over the protein surface. These values were calculated using coordinates from the Protein Data Bank with the exception of metmyoglobin, 10T, cS82R and β -trypsin. For these structures, coordinates were not available and the values quoted are taken from the literature. For β -galactosidase the values quoted are averages based on several crystals and structures all determined using the same detector (R-Axis IV).

structure and dynamics has been studied in several systems,^{5-7,10,11,20,21} while study of the cooling process *per se* has mainly focused on improving techniques.²²⁻³⁰ However, there has yet to be a clear explanation for the unit cell contraction, which appears to be fairly universal among protein crystals.

Whether cryogenic techniques provide an accurate description of macromolecular structure and interaction at biologically relevant temperatures remains an open question. Here we explore the unit cell contraction and discuss its implications for the study of interactions between macromolecules *via* low-temperature crystallography.

Results and Discussion

Reversible unit cell contraction and repacking

Escherichia coli β -galactosidase is a homotetramer of 460 kDa. Its structure has been determined at room temperature in a monoclinic crystal form and at both room temperature and 100 K using crystals from an orthorhombic space group.^{31,32} In the process of collecting data on inhibitor complexes and other variants we noticed that the low-temperature crystals had unit cell volumes about 6% smaller

than at room temperature (Figure 1), consistent with protein crystals in general. Further experiments showed that this unit cell change is reversible (Figure 2).

The unit cell contraction requires that the centers-of-mass of the protein molecules move closer together. This could occur either by contraction of the protein or repacking of the crystal. Comparison of the refined coordinates of the low and room-temperature models suggested that there are localized changes of surface side-chains and some small domain shifts but the overall fold is unchanged and the protein itself contracts by only 1-2% on flash cooling^{2,4-18} (see below). This led us to consider repacking as the source of the unit cell contraction.

The role of long polar side-chains

To investigate repacking we first calculated the area of the protein molecule involved in lattice contacts (see Figure 3 for details). This changes from $4180(\pm 50) \text{ \AA}^2$ at room temperature to $6130(\pm 390) \text{ \AA}^2$ on cooling. In achieving this approximately 50% increase in contact area the tetramer rotates by 3° with concomitant relative motions of 3-4 \AA at some of the lattice contacts.

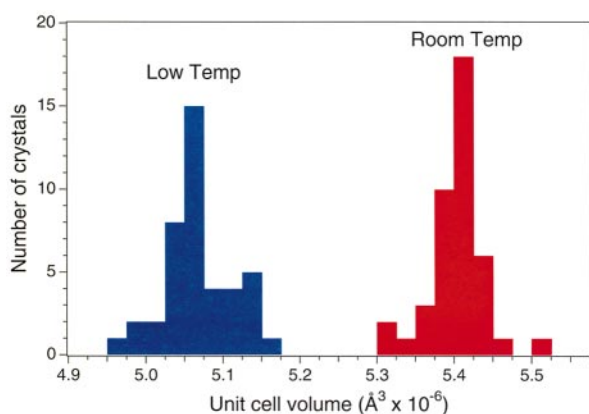


Figure 1. Histogram showing the unit cell volumes for different crystals of β -galactosidase. The crystal form is in space group $P2_12_12_1$ with cell dimensions $a = 149.6 \text{ \AA}$, $b = 168.4 \text{ \AA}$, $c = 200.7 \text{ \AA}$ at low temperature.³² The Figure includes data for three point mutants and a number of different inhibitor complexes. The solvent conditions also vary somewhat, especially for the room temperature crystals. Despite these variations, the unit cell of the low-temperature crystals is about 6% smaller than that at room temperature (5.2% smaller than at room temperature in the cryobuffer).

Figure 3(a) and (b) show the buried area for each type of amino acid at the lattice contacts. Clearly the increase in lattice contact area on freezing is dominated by the long, polar, side-chains. Indeed, of the overall increase of 2000 \AA^2 in lattice contact area, 68% comes from the four amino acids Glu, Gln, Lys and Arg. The fact that these amino acids (plus methionine) have the greatest number of rotatable bonds suggests that the reason for the lattice contraction is entropic in nature. The lattice contacts are comprised of regions on the protein surface with varying degrees of order, and include both solvent molecules and protein side-chains. When the crystal is cooled some of these disordered regions become ordered. In the case of β -galactosidase, the effect is quite dramatic. At higher temperatures the side-chains with most degrees of freedom are entropically the least likely to be ordered in a lattice contact. Indeed, at room temperature these are under-represented at the lattice contacts in comparison to the distribution of surface residues in the isolated tetramer (Figure 3(a)). At low temperature, however, it becomes thermodynamically easier to order these residues, and similarly, surface-associated solvent molecules. The low-temperature packing arrangement is then a result of side-chain and solvent ordering, increased intermolecular interactions and a more intimate association between neighboring molecules in the crystal. Figure 4 shows a particularly striking example in which several long polar side-chains are poorly ordered at room temperature. Upon cooling these side-chains become more ordered and make specific interactions with both

protein atoms and ordered solvent molecules. Further, the neighboring tetramers move about 3 \AA closer together at this location to form additional lattice contacts. There are other examples of this sort at other places in the crystal.

The reversibility of the repacking (Figure 2(b)) suggests flexibility of the crystal lattice, allowing it to explore alternative conformations on the flash-cooling time-scale (~ 0.1 -1 second). Lowering the temperature to 100 K appears to create a new free energy minimum for the crystal in which the long polar side-chains are more involved in the lattice contacts. Whether this is the global free energy minimum for the crystal at 100 K is unclear, and is probably inaccessible to experiment, as it would require crystal growth at 100 K where the bulk solvent is vitrified. At room temperature the packing distribution is more narrow than at low temperature, perhaps because the molecules are more free to seek the overall free energy minimum. Although the temperature decrease facilitates the ordering of surface side-chains, it remains unclear whether such ordering is a cause for, or an effect of, the unit cell contraction. To address this question we examined the response of the other major component of the crystal, the bulk solvent, to the decrease in temperature.

The role of bulk solvent

When a protein crystal is flash-cooled and the solvent scattering appears as a diffuse ring, it suggests that vitrification has occurred. The presence of sharper rings indicates that the bulk solvent has formed microcrystals. In the case of β -galactosidase the cryosolvent consists of 70% (v/v) mother liquor (100 mM bis-Tris (pH 6.5), 200 mM MgCl_2 , 100 mM NaCl, 10 mM dithiothreitol and 10% (w/v) polyethylene glycol 8000) plus 30% (v/v) dimethylsulfoxide (DMSO). Using a buoyancy-based technique with liquid nitrogen as the displaced fluid (see Methods) we measured the density of this vitrified liquid at 77 K as $1.157(\pm 0.002) \text{ g cm}^{-3}$. This is 7.5% higher than the density of the same liquid at room temperature ($1.076(\pm 0.002) \text{ g cm}^{-3}$). If the mother liquor alone is flash-cooled it does not vitrify and its density decreases by 3.5% (from $1.042(\pm 0.002) \text{ g cm}^{-3}$ to $1.006(\pm 0.005) \text{ g cm}^{-3}$). Bulk solvents with other cryoprotectants such as glycerol or sucrose show similar behavior (unpublished results).

Both of the effects described, surface side-chain ordering and bulk solvent contraction, will tend to make the unit cell contract. Whether one effect dominates is unclear, but the interplay between the two is likely to determine the outcome of cryocooling. A useful quantity to consider in this context is v_{exit} , the volume fraction of bulk solvent that exits the crystal on cooling. This can readily be shown to be:

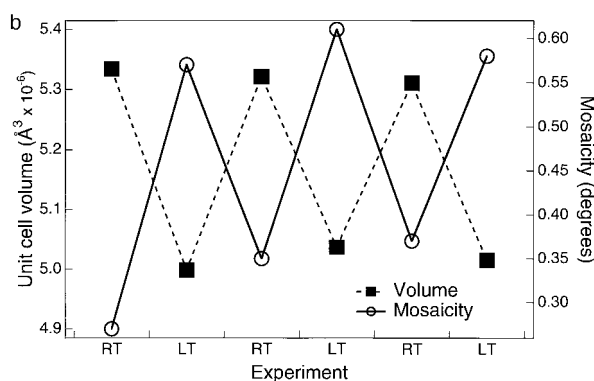
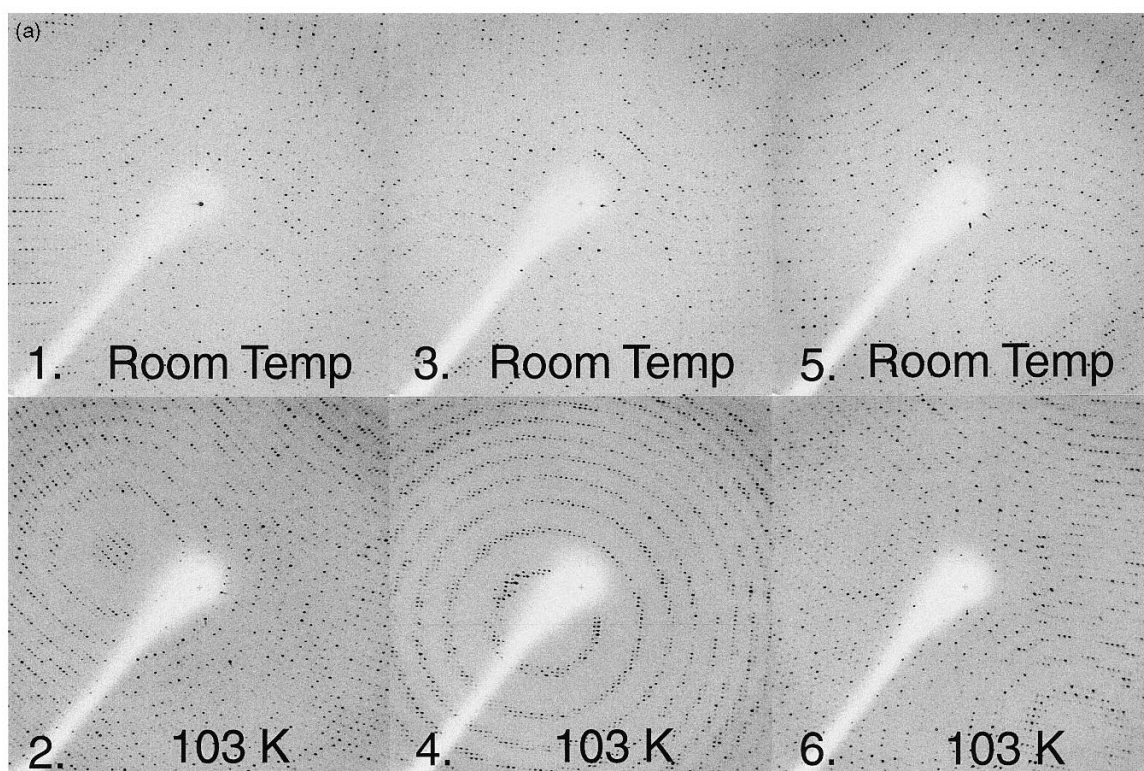


Figure 2. (a) Diffraction images from a single crystal of β -galactosidase recycled between room and low temperature. The crystal was alternatively mounted in a capillary tube for the room-temperature exposures and in a small loop for the low-temperature experiments. It was flash-frozen by rapid introduction into the cold stream and “flash melted” by immersion in a drop of mother liquor on a cover-slip while still in the cold stream. The resolution in the corner is 3.5 Å. (b) Graph showing the reversible change in unit cell volume and mosaicity with freezing. These parameters were determined with postrefinement in Mosflm^{49–51} using several images 90° apart.

$$v_{\text{exit}} = \Delta_{\text{sol}} + (v_{\text{prot}}\Delta_{\text{prot}} - \Delta_{\text{cell}})(1 - \Delta_{\text{sol}})/(1 - v_{\text{prot}}) \quad (1)$$

where Δ_{sol} is the fractional change in volume of the bulk solvent on cooling, Δ_{cell} is the fractional change in volume of the unit cell on cooling, Δ_{prot} is the fractional change in volume of the protein on cooling and v_{prot} is the fraction of the unit cell volume at room temperature that is occupied by protein. (v_{prot} can be estimated as $1.23/V_{\text{M}}$ where V_{M} is the crystal packing parameter.³³) For the crystals of β -galactosidase $v_{\text{prot}} = 0.43$. If the unit cell contraction were driven solely by the solvent

contraction, v_{exit} would be expected to be zero. Using the observed values of -5.2% for Δ_{cell} , -7.5% for Δ_{sol} , -1.0% for Δ_{prot} and 0.43 for v_{prot} we find that v_{exit} is 1-2%. This marginally positive value suggests that at least part of the unit cell contraction is driven by the entropic considerations described earlier, forcing 1-2% of the bulk solvent to exit the crystal. It is, however, likely that the constraining environment of the solvent channels perturbs at least some of the bulk solvent from its bulk behavior.³⁴ Such perturbation may be responsible for the slight deviation from zero. In either case, the role of the cryoprotectant may, in part, be

Table 2. Temperature-dependent changes in protein crystal structures

Protein	PDB code		Resolution (Å)		Mol. mass (kDa)	Change in backbone (Å)	ΔR_g (%)	Rotation (deg.)	Intramolecular contacts			Intermolecular contacts		
	RT	LT	RT	LT					Number, RT	Increase (%)	Retained (%)	Number, RT	Increase (%)	Retained (%)
Plastocyanin	1PLC	1PNC	1.3	1.6	10.5	0.35	-0.65	1.5	320	19	83	56	39	75
RNase A	9RAT	1RAT	1.5	1.5	13.7	0.30	-0.61	0.4	502	15	76	100	0	58
HEWL (Kurinov)	1LSE	1LSF	1.7	1.7	14.3	0.54	-0.77	2.3	590	14	70	91	33	54
HEWL (Young)	6LYT	5LYT	1.9	1.9	14.3	0.48	-0.97	1.3	611	22	68	103	23	46
HEWL (MonoA)	4LYT(a)	3LYT(a)	1.9	1.9	14.3	0.59	-0.78	2.8	637	15	60	134	13	28
HEWL (MonoB)	4LYT(b)	3LYT(b)	1.9	1.9	14.3	0.79	+0.03	1.6	629	7	52	152	32	44
Flavodoxin	2FX2	3FX2	1.9	1.9	15.7	0.33	-0.91	1.0	528	36	84	56	46	57
IL1 β	-	-	2.0	1.5	17.1	0.62	-0.41	1.5	510	8	63	172	19	44
Metmyoglobin	1MBN	-	2.0	-	17.2	-	-0.98	-	-	-	-	-	-	-
T4L	1L63	-	1.8	1.1	18.4	0.35	-0.68	1.1	756	6	82	106	21	57
α -Lytic protease	2ALP	1TAL	1.7	1.5	19.9	0.15	-0.13	0.6	712	2	90	70	6	80
λ B-crystallin	4GCR	1GCS	1.5	2.0	21.0	0.31	-0.56	0.3	766	13	72	142	31	56
Trypsinogen	1TGC	2TGT	1.8	1.7	23.3	0.21	-0.09	0.7	537	2	85	60	-7	67
β -Trypsin	1TLD	-	1.5	-	23.3	-	-0.62	-	-	-	-	-	-	-
Trypsin	1ANE	1DPO	2.2	1.6	23.8	0.21	-0.25	0.9	791	16	78	82	10	63
β -Lactamase	1BLC	3BLM	2.2	2.0	28.8	0.38	-0.53	3.6	1110	29	75	82	50	34
10 t	-	1XAA	-	2.1	36.8	-	-0.15	-	-	-	-	-	-	-
cS82R	-	1XAC	-	2.1	37.0	-	-0.49	-	-	-	-	-	-	-
β -Galactosidase	1HN1	1DP0	3.0	1.7	458.8	0.55	-0.50	3.1	22100	-14(3)	59(62)	68	47(51)	21(22)

RT is room temperature and LT is low temperature. The PDB codes and maximal resolution for the structures analyzed are given. A dash indicates that the structure has not been deposited in the PDB. Change in backbone is the root-mean-square deviation of main-chain atoms after optimal superposition. Rotation is the rotation in degrees to give this superposition. The translation is not given because its magnitude depends on the location of molecule relative to the origin. ΔR_g is the fractional change in the radius of gyration with cooling. Intramolecular contacts are those between different residues in the same molecule. Intermolecular contacts are those between different molecules (across crystal contacts). Two atoms are considered to be in contact when their center-to-center distance is less than the sum of their van der Waals radii plus 0.25 Å. Increase (%) and retained (%) refers to the increase and retention of contacts with cryocooling. The change in number of contacts can have two causes: (1) contraction of the molecule and crystal; (2) change in coordinate error (due to a change in resolution limit). In the case of β -galactosidase, the disparity in resolution limit between RT and LT is quite large (3.0 Å *versus* 1.7 Å). Although the molecule contracts (as measured by α , Table 1), the number of contacts decreases, due to more reliable positioning of the atoms with a fivefold increase in the amount of data. We therefore also report contact data (in parentheses) for 1DP0 after refinement using data to only 3.0 Å resolution.

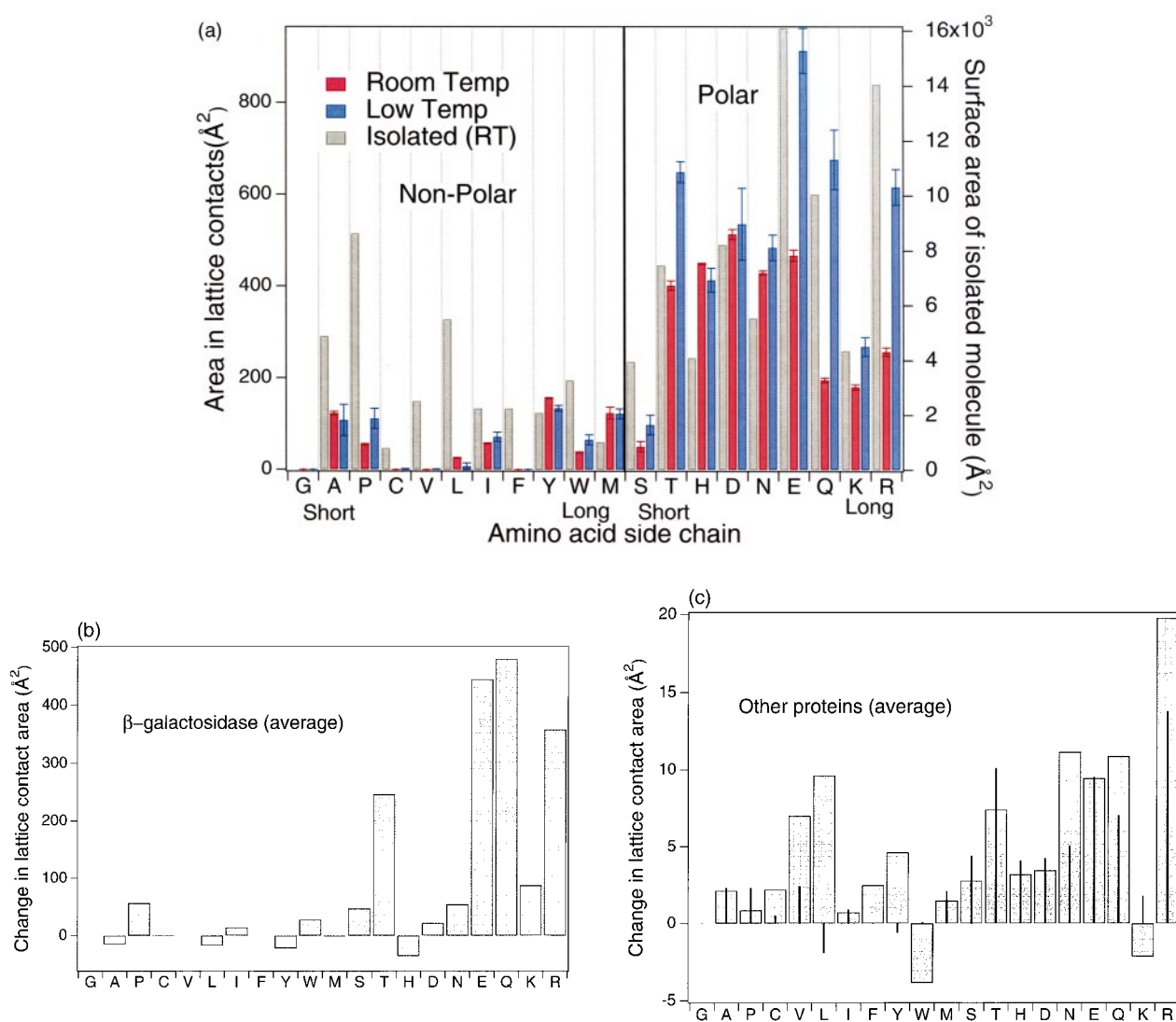


Figure 3. (a) Bar graph showing the area contributed to lattice contacts by the different amino acid side-chains in β -galactosidase (left axis). Using the program EDPDB^{43,44} with a probe radius of 1.4 Å, we first determined the surface area of side-chains exposed to solvent for a molecule of β -galactosidase isolated from the crystal lattice. The results are shown in gray with the scale on the right side of the Figure. The calculation was then repeated for the β -galactosidase molecule incorporated within, respectively, the room-temperature and flash-frozen crystals. The neighboring molecules in the lattice were determined with WHATIF.⁴⁵ The decrease in surface area is attributed to lattice contacts. Values for the room temperature crystals are shown in red and for the frozen crystals in blue. The scale is at the left. The error bars are ± 1 standard deviation based on 19 low-temperature structures and four at room-temperature. These include various inhibitor complexes, structures of point mutants and structures determined under different solvent conditions. The low-temperature structures range in resolution from 3.0 to 1.7 Å, while those at room temperature are at about 3.0 Å resolution. (b) Temperature-dependent contributions of the different amino acids to crystal contacts in β -galactosidase. The values plotted are the differences between the blue and red histograms in (a). Each entry shows the amount by which the crystal contact area generated by a given type of amino acid changes on flash-cooling. (c) Temperature-dependent contributions of the different amino acids to crystal contacts in smaller proteins. The Figure was calculated in the same way as (b), averaging over the crystal contacts of all the structures in Table 1 (except β -galactosidase) for which the coordinates are available. The outliers (especially V and L) are mainly due to HEWL. The data set without HEWL is plotted as thin dark lines.

to ameliorate mechanical damage due to a large v_{exit} , which would be 12% in the case of the unvitrified bulk solvent. This solvent transport may also be part of the reason that smaller crystals tend to freeze with less damage than larger ones. Another approach to minimize solvent expansion was used to freeze myoglobin crystals, and

involves the use of pressure prior to freezing in order to form ice III, which contracts relative to water, rather than ice I, which forms at atmospheric pressure and expands.³⁵

In cases where there is no obvious cryoprotectant, it is uncertain what happens to the bulk solvent. Pure water can be vitrified only in micro-

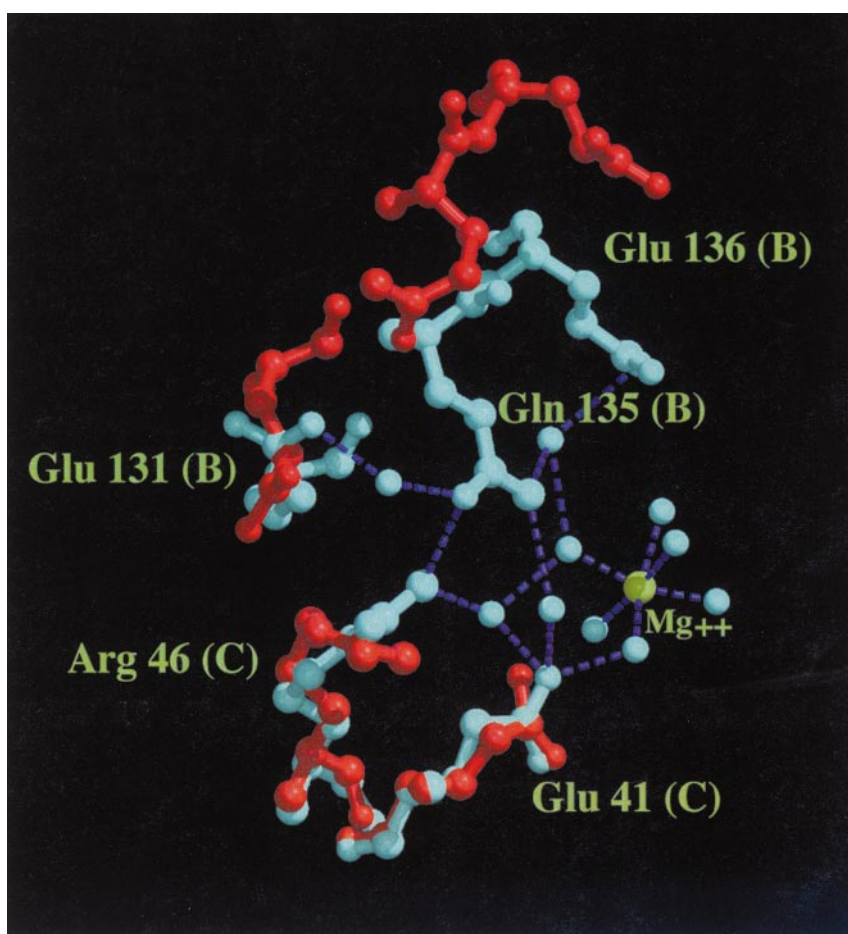


Figure 4. An example of side-chain ordering at a lattice contact on freezing. Coordinates are from the refined models for room-temperature and low-temperature β -galactosidase (ref. 32 and PDB codes 1HN1 and 1DP0). Atoms in the room-temperature structure are colored red and the low-temperature structure cyan. Side-chains in one molecule of β -galactosidase are labeled B and in the neighboring molecule C. At room temperature the five side-chains are poorly ordered with average B -factors of about 140 \AA^2 . On freezing the main-chain atoms move 3 \AA closer together and the side-chains become ordered with average B -factors of about 30 \AA^2 . With the participation of solvent molecules and a putative Mg^{2+} (in green), they generate a region of crystal contact much more extensive than that seen at room temperature. Because the low-temperature structure is to much higher resolution (1.7 \AA) than that at room temperature (3.0 \AA), we repeated the low-temperature refinement with the synchrotron data set truncated at 3.0 \AA and also with a 3.0 \AA resolution data set collected on a home source. In both cases the residues are less well defined than with 1.7 \AA resolution data. However, the

region is still seen to be more ordered than the room-temperature structure (average side-chain B -factors of 45 \AA^2 and 75 \AA^2 versus 140 \AA^2 for room temperature). This confirms that the differences seen in the room-temperature and low-temperature models are not simply due to differences in the resolution of the data.

metre-sized droplets and, even then, the density decreases by 6%.^{36–38} Such solvent expansion would require the unit cell contraction be driven solely by the entropic effects, and would lead to a large v_{exit} . Possibly some protein crystals have the mechanical stability, or the presence of suitable channels to the surface, that permit larger values of v_{exit} .

Generality and implications

In a pioneering study Frauenfelder and co-workers^{10,11} investigated the temperature-dependence of crystalline metmyoglobin. They observed that the unit cell volume decreased by 5% on cooling, very much in line with subsequent studies of other protein crystals. They also found a 3% change in the volume of the protein on cooling, which is at the high end of the 1–3% range subsequently found with other proteins (see Tables 1–3 for additional details). In all cases reported, the unit cell contracts more than the individual protein molecules, requiring repacking.

To gain a more general view of cryocooling-induced repacking we conducted a survey of those structures for which we could find both room-temperature and low-temperature coordinates (14 in all). The results are summarized in Tables 1–4. As shown in Table 2, the overall structures of proteins at room temperature and at low temperature are quite similar with root-mean-square differences between main-chain atoms averaging about 0.5 \AA . As seen by the decrease in the radius of gyration, all the structures contract somewhat. They also rotate to varying degrees, the larger rotations being correlated with reorganization of the crystal contacts (see below).

As also shown in Table 2, in almost all cases the number of intermolecular contacts (i.e. crystal contacts) as well as intramolecular contacts increases with cryocooling, reflecting the overall contraction of both the molecule and the crystal. To determine the degree to which the different interfaces are remodeled upon cooling, we determined the fraction of room-temperature contacts which are retained. For the intramolecular contacts, this fraction ranges from 0.9 (α -lytic protease) to 0.5 (hen

Table 3. Hierarchical contacts of β -galactosidase

	Contacts at interface				Polarity of interface (%)	Density of H-bonds	Change in contact area due to bridging water (%)
	Number, RT	Increase (%)	Retained (%)				
Crystal interface	68	51	22	61	0.44	13.8	
Subunit interface	415	20	55	47	1.02	6.9	
Domain interface	1604	5	58	44	1.34	6.0	
Intradomain	18,798	2	62	40	2.05	2.9	

Low-temperature contact data are based on the refinement of 1DP0 using data to only 3.0 Å resolution (see Table 2). The rest of the Table is based on the high-resolution structure. The polarity of the interface is the percentage of the interface area that is made up of polar atoms (N or O). The density of H-bonds is the number of hydrogen bonds per 100 Å² of polar interface area. For the intradomain surface the reference state is the fully extended model of the polypeptide chain. A bridging water molecule is less than 3.2 Å from each of two atoms which are themselves at least 4.0 Å apart. These were then assigned to one interface and the area of the second interface buried by the first was calculated, both with and without the bridging water molecules. The increase in buried area due to the bridging water molecules is reported.

egg white lysozyme, HEWL) suggesting different degrees of remodeling within the protein molecules. For the intermolecular (crystal) contacts, the spread is larger, ranging from 0.8 (α -lytic protease) to 0.2 (β -galactosidase). Thus, with some protein crystals, the crystal contacts change very little while others change dramatically. But, on average, the intermolecular interactions change more than the intramolecular interactions. (As a control we also compared two low-temperature β -galactosidase structures with nearly identical cell dimensions. In this case the “contacts retained” was about 90% (data not shown), which probably represents the upper limit for structures refined at about 1.8 Å resolution.)

Because β -galactosidase is so much larger than the other proteins the contacts in this case were further broken down into intertetramer (crystal contacts), intersubunit, interdomain and intradomain contacts (Table 3). Descending this hierarchy, two trends are observed with regard to cooling. First, the fractional increase in contacts gets smaller, and second, the fraction of retained contacts gets larger. Earlier analysis of β -galactosidase showed that while the interfaces higher in the hierarchy are more hydrophilic in nature, hydrogen bonding is less important.^{32,39} Table 3 also shows that bridging water molecules are more prevalent higher in the hierarchy. Taken together this suggests that while all interfaces are likely to be perturbed somewhat by cooling, those higher in the hierarchy (i.e. crystal contacts and subunit interfaces) are more loosely organized, less stable and are likely to be perturbed to a greater degree on cooling.

In Table 4, the amino acids are considered based on side-chain solvent accessibility and on participation in crystal contacts. Overall, contact residues have higher *B*-factors than non-contact residues, whether they are buried or on the surface. This is true at both room temperature (Table 4) and low temperature (not shown). There is a very slight tendency for contact residues to undergo larger *B*-factor decreases upon cooling than non-contact residues, although this might be expected, since

the contact residues generally have higher *B*-factors. We also determined the changes in side-chain dihedral angles. Although these data are noisy, the general result is that, on average, χ_1 (Table 4) and χ_2 (not shown) undergo greater changes if the residues are involved in crystal contacts. Taken together, the analysis suggests that upon cryocooling both intramolecular and intermolecular contact interfaces are likely to be perturbed, but that the changes tend to be more dramatic in the latter case. There is also some indication that non-contact surface residues undergo smaller changes than those involved in crystal contacts.

Table 3 summarizes in more detail the contraction of the molecule and the crystal. In the interior of a protein molecule the side-chains are usually quite well ordered. Occasional solvent molecules are observed within proteins and are also usually well ordered. The atoms within the well-packed core of a protein are expected to move slightly closer together on cooling due to the anharmonic nature of the interatomic potential functions.⁴⁰ The average linear thermal expansion coefficient for the proteins listed in Table 1 is $61 \times 10^{-6} \text{ K}^{-1}$, somewhat higher than for NaCl ($40 \times 10^{-6} \text{ K}^{-1}$),¹⁹ the same as liquid water ($70 \times 10^{-6} \text{ K}^{-1}$)¹¹ and substantially less than ethanol or benzene ($\sim 400 \times 10^{-6} \text{ K}^{-1}$).¹¹ Although the core of a protein is often thought of as hydrocarbon-like, it is clear that a liquid hydrocarbon is a poor model with regard to thermal expansion. This is, however, to be expected, since the protein is restricted by covalent bonds along the backbone which tend to decrease thermal expansion relative to free ethanol or benzene. Because of this restrained packing, substantial reordering of the atoms within a protein on cooling is unlikely.

On the surface of the protein, however, the situation is different. Side-chains, especially the longer ones, are often partially or completely disordered. It can be estimated that the entropy cost of restricting rotation about a single bond at room temperature is about $0.6 \text{ kcal mol}^{-1}$.⁴¹ At 100 K this will be reduced to $0.2 \text{ kcal mol}^{-1}$. Similarly, the entropy cost of localizing solvent molecules will also be

Table 4. Classification of residues in different proteins and their behavior on cooling

Protein	Partitioning of residues				Surface in crystal contacts (%)	$\langle B_{RT} \rangle$ (\AA^2)				$\langle B_{RT} - B_{LT} \rangle$ (\AA^2)				Average change in χ_1			
	Buried		Surface			Buried		Surface		Buried		Surface		Buried		Surface	
	Non-contact	Crystal contact	Non-contact	Crystal contact		Non-contact	Crystal contact	Non-contact	Crystal contact	Non-contact	Crystal contact	Non-contact	Crystal contact	Non-contact	Crystal contact	Non-contact	Crystal contact
Plastocyanin	27	21	20	31	47	10	15	15	23	-6	-9	-8	-12	3	4	17	17
RNase A	46	13	30	35	25	11	15	25	27	-7	-10	-8	-15	15	40	23	19
HEWL (Kurinov)	43	20	39	27	39	20	18	26	29	-1	0	1	-1	11	5	21	37
HEWL (Young)	42	18	42	27	42	12	12	19	22	-5	-5	-11	-11	18	11	17	39
HEWL (MonoA)	49	18	25	37	30	15	18	21	24	-10	-9	-14	-14	26	19	56	34
HEWL (MonoB)	45	24	26	34	31	13	18	16	20	-8	-8	-8	-10	18	44	28	47
Flavodoxin	55	22	53	17	24	17	21	32	25	-6	-7	-12	-7	10	14	22	19
IL1 β	46	26	48	30	27	32	40	69	71	-15	-16	-26	-24	14	8	34	33
T4L	52	34	54	22	28	19	21	42	46	-5	-6	-19	-24	4	9	12	19
α -Lytic protease	69	27	78	24	23	10	12	18	23	-6	-7	-11	-15	3	4	5	12
λ B-crystallin	57	27	37	53	33	13	20	26	31	-4	-5	-7	-7	7	8	12	18
Trypsinogen	68	16	55	25	20	13	16	20	19	-4	-6	-7	-4	5	3	9	11
Trypsin	92	19	87	25	20	11	14	26	19	-5	-5	-9	-6	14	5	19	21
β -Lactamase	123	28	69	37	23	18	22	30	31	-3	-4	-7	-7	15	27	30	35
β -Galactosidase	2174	28	1741	101	3	33	42	56	72	-18	-19	-24	-31	14	16	21	25
Average						17	20	29	32	-7	-8	-11	-13	11	12	17	21

Residues were partitioned into buried and surface and, within these categories, into crystal contact and non-contact. A residue was considered to be buried if less than 20% of its side-chain was accessible to solvent in the isolated, room-temperature crystal. The remaining residues were considered to be surface. $\langle B_{RT} \rangle$ is the mean side-chain B -factor for atoms in the various residue classes in the room-temperature crystal structure. $\langle B_{RT} - B_{LT} \rangle$ is the change in the B -factor with cooling.

reduced. Thus, as the protein is cooled it becomes favorable for the longer side-chains to form specific interactions, drastically reducing their effective volumes. Such changes are practically impossible within the molecule, since the side-chains are already ordered at room temperature. Therefore, this effect is more likely to play a role in inter- rather than intramolecular interactions and the lattice contracts more than the protein itself (on average $\alpha_{\text{cell}}/\alpha_{\text{prot}} = 3.2$; Table 1). The importance of a disordered boundary layer to the bulk viscoelastic properties of protein crystals and films has also been discussed by Morozov & Gevorkian.²⁰

Figure 3(c) shows, in aggregate, how cooling affects the crystal contacts for the various proteins in Table 1. The result is tolerably similar to that for β -galactosidase (Figure 3(b)), suggesting that the behavior is general. The outliers on the non-polar side of the graph (primarily valine and lysine) are due to just a few residues in HEWL and, since there are four copies of HEWL in the data set, these outliers are somewhat magnified. The thin dark lines show the result when the four HEWL structures are excluded. Dasgupta *et al.*⁴² have previously noted that lysine residues, although common on the surface of most proteins, are disfavored and under-represented in the formation of intermolecular crystal contacts. The present results are consistent with this finding and also suggest that although lysine side-chains are long and polar they do not tend to form intermolecular contacts on cooling in the manner observed for Glu, Gln and Arg.

We examined two smaller proteins in detail, T4 lysozyme and IL1 β . Both show more subtle packing changes than those observed with β -galactosidase. Nevertheless, these changes involve ordering side-chains (and main-chain for IL1 β) near crystal contacts at low temperature, permitting interactions to form which appear to draw the molecules closer together. Upon heating, some of these interactions are broken, allowing these side-chains to occupy a larger effective volume, and the crystal expands.

These results are relevant to macromolecular interactions in general. The cooling-induced repacking observed here illustrates how intermolecular interactions can be modulated by temperature. Crystals of macromolecules or macromolecular complexes are typically grown in the temperature range 4–20 °C and then flash-frozen. Under such conditions the overall architecture of the higher-temperature structure is likely to be maintained. Similarly, extensive intermolecular interfaces responsible for high-affinity binding are likely to be only slightly perturbed by cooling. However, more tenuous interfaces indicative of weaker, more transient intermolecular interactions may be significantly affected. Such interfaces may become more relevant in the future as various signaling pathways are studied in more detail. It is possible that specific interactions seen in such low-temperature crystal structures, especially those

involving long flexible side-chains, and which may appear to contribute to protein-protein or protein-nucleic acid binding, may be of questionable relevance at room temperature.

Methods

Crystallography and cryo-cooling

Crystallization and refinement of orthorhombic β -galactosidase structures was as described.³²

To test reversibility of freezing, a crystal pre-equilibrated in cryosolvent (30% DMSO, 70% mother liquor, where mother liquor is 100 mM bis-Tris (pH 6.5), 10% PEG 8000, 200 mM MgCl₂, 100 mM NaCl, 10 mM DTT and the ligand of interest) was mounted in a glass capillary and several X-ray exposures 90° apart were taken with an in-house X-ray source at room temperature (total exposure time ~one hour). The crystal was then expelled from the capillary and flash-frozen in the cold stream using a cryo-loop (Hampton). After taking several exposures similar to those at room temperature the crystal was “flash melted” by rapidly placing it in a large drop of cryosolvent on a coverslip. It was then remounted in a capillary for room temperature analysis. This cycle was repeated as many times as possible. The limiting factor appeared to be repeated handling.

Coordinate analysis

Solvent-accessible surface area was determined using EDPDB.^{43,44} The area buried at crystal contacts was determined by calculating the accessible area of an isolated β -galactosidase tetramer and then subtracting the solvent-accessible surface area of the tetramer in the crystals, either at room temperature or flash-frozen. The neighboring molecules in the crystal were determined with WHATIF.⁴⁵ Dihedral angles were calculated with *bbdep*.⁴⁶ Other calculations involving contacts, bridging water molecules, and *B*-factor and dihedral angle changes were carried out using EDPDB, WHATIF and unpublished programs by the authors.

Macroscopic density measurements

The density of the mother liquor at room temperature was determined with a volumetric flask and an analytical balance. To measure the density at cryogenic temperature, a buoyancy-based technique with liquid nitrogen as the displaced liquid was used.⁴⁷ Briefly, a small amount of mother liquor (0.5–1.0 ml) was placed in a plastic tube and weighed with an analytical balance both in air and when submerged in liquid nitrogen. Similar measurements with the tube empty allowed the buoyant force on the tube alone to be determined. Given the known density of liquid nitrogen it is straightforward to calculate the density of the vitrified mother liquor at liquid nitrogen temperature (77 K) and thus the density change upon cryocooling. The low-temperature density determination was repeated many times to ensure that the frozen cryosolvent had vitrified (indicated by its clear appearance) and that the overall procedure gave reproducible results.

Acknowledgments

We thank Drs Blaine Mooers and Michael Quillin both for access to unpublished data on T4 lysozyme and interleukin-1 β and, together with Drs Enoch Baldwin, Richard Kingston, Walt Baase, Jim Remington and Bill Girard for helpful discussions. We also thank both the Stanford Synchrotron Radiation Laboratory and the Lawrence Berkeley Advanced Light Source for essential help with data collection. This work was supported, in part, by NIH grant GM20066 to B.W.M.

References

- Hope, H. (1988). Cryocrystallography of biological macromolecules: a generally applicable method. *Acta Crystallog. sect. B*, **44**, 22-26.
- Haas, D. J. & Rossmann, M. G. (1975). Crystallographic studies on lactate dehydrogenase at -75°C . *Acta Crystallog. sect. B*, **26**, 998-1004.
- Teng, T.-Y. & Moffat, K. (1998). Cooling rates during flash cooling. *J. Appl. Crystallog.* **31**, 252-257.
- Fields, B. A., Bartsch, H. H., Bartunik, H. D., Cordes, F., Guss, J. M. & Freeman, H. C. (1994). Accuracy and precision in protein crystal structure analysis: two independent refinements of the structure of poplar plastocyanin at 173 K. *Acta Crystallog. sect. D*, **50**, 709-730.
- Tilton, R. F., Jr, Dewan, J. C. & Petsko, G. A. (1992). Effects of temperature on protein structure and dynamics: X-ray crystallographic studies of the protein ribonuclease-A at nine different temperatures from 98 to 320 K. *Biochemistry*, **31**, 2469-2481.
- Kurinov, I. V. & Harrison, R. W. (1995). The influence of temperature on lysozyme crystals. Structure and dynamics of protein and water. *Acta Crystallog. sect. D*, **51**, 98-109.
- Young, A. C., Tilton, R. F. & Dewan, J. C. (1994). Thermal expansion of hen egg-white lysozyme. Comparison of the 1.9 Å resolution structures of the tetragonal form of the enzyme at 100 K and 298 K. *J. Mol. Biol.* **235**, 302-317.
- Young, A. C. M., Dewan, J. C., Nave, C. & Tilton, R. F. (1993). Comparison of radiation-induced decay and structure refinement from X-ray data collected from lysozyme crystals at low and ambient temperatures. *J. Appl. Crystallog.* **26**, 309-319.
- Watt, W., Tulinsky, A., Swenson, R. P. & Watenpaugh, K. D. (1991). Comparison of the crystal structures of a flavodoxin in its three oxidation states at cryogenic temperatures. *J. Mol. Biol.* **218**, 195-208.
- Parak, F., Hartmann, H., Aumann, K. D., Reuscher, H., Rennekamp, G., Bartunik, H. & Steigemann, W. (1987). Low temperature X-ray investigation of structural distributions in myoglobin. *Eur. Biophys. J.* **15**, 237-249.
- Frauenfelder, H., Hartmann, H., Karplus, M., Kuntz, I. D., Jr, Kuriyan, J., Parak, F. *et al.* (1987). Thermal expansion of a protein. *Biochemistry*, **26**, 254-261.
- Rader, S. D. & Agard, D. A. (1997). Conformational substates in enzyme mechanism: the 120 K structure of alpha-lytic protease at 1.5 Å resolution. *Protein Sci.* **6**, 1375-1386.
- Lindley, P., Najmudin, S., Bateman, O., Slingsby, C., Myles, D., Kumaraswamy, V. S. & Glover, I. (1993). Structure of bovine γ B-crystalline at 150 K. *J. Chem. Soc. Faraday Trans.* **89**, 2677-2682.
- Walter, J., Steigemann, W. & Singh, T. P. (1982). On the disordered activation domain in trypsinogen: chemical labelling and low-temperature crystallography. *Acta Crystallog. sect. B*, **38**, 1462-1472.
- Nakasako, M. (1999). Large-scale networks of hydration water molecules around bovine beta-trypsin revealed by cryogenic X-ray crystal structure analysis. *J. Mol. Biol.* **289**, 547-564.
- Earnest, T., Fauman, E., Craik, C. S. & Stroud, R. (1991). 1.59 Å structure of trypsin at 120 K: comparison of low temperature and room temperature structures. *Proteins: Struct. Funct. Genet.* **10**, 171-187.
- Nagata, C., Moriyama, H., Tanaka, N., Nakasako, M., Yamamoto, M., Ueki, T. & Oshima, T. (1996). Cryocrystallography of 3-isopropylmalate dehydrogenase from *Thermus thermophilus* and its chimeric enzyme. *Acta Crystallog. sect. D*, **52**, 623-630.
- Chen, C. C., Smith, T. J., Kapadia, G., Wäsch, S., Zawadzke, L. E., Coulson, A. & Herzberg, O. (1996). Structure and kinetics of the β -lactamase mutants S70A and K73H from *Staphylococcus aureus* PC1. *Biochemistry*, **35**, 12251-12258.
- Rubin, T., Johnston, H. L. & Altman, H. W. (1961). Thermal expansion of rock salt. *J. Phys. Chem.* **65**, 65-68.
- Morozov, V. & Gevorkian, S. (1985). Low-temperature glass transition in proteins. *Biopolymers*, **24**, 1785-1799.
- Rasmussen, B. F., Stock, A. M., Ringe, D. & Petsko, G. A. (1992). Crystalline ribonuclease A loses function below the dynamical transition at 220 K. *Nature*, **35**, 423-424.
- Petsko, G. A. (1975). Protein crystallography at sub-zero temperatures: cryo-protective mother liquors for protein crystals. *J. Mol. Biol.* **96**, 381-392.
- Mitchell, E. P. & Garman, E. F. (1994). Flash freezing of protein crystals: investigation of mosaic spread and diffraction limit with variation of cryoprotectant concentration. *J. Appl. Crystallog.* **27**, 1070-1074.
- Garman, E. F. & Schneider, T. R. (1997). Macromolecular crystallography. *J. Appl. Crystallog.* **30**, 211-237.
- Harp, J. M., Timm, D. E. & Bunick, G. J. (1998). Macromolecular crystal annealing: overcoming increased mosaicity associated with cryocrystallography. *Acta Crystallog. sect. D*, **54**, 622-628.
- Yeh, J. I. & Hol, W. G. J. (1998). A flash-annealing technique to improve diffraction limits and lower mosaicity in crystals of glycerol kinase. *Acta Crystallog. sect. D*, **54**, 479-480.
- Harp, J. M., Hanson, B. L., Timm, D. E. & Bunick, G. J. (1999). Macromolecular crystal annealing: evaluation of techniques and variables. *Acta Crystallog. sect. D*, **55**, 1329-1334.
- Garman, E. (1999). Cool data: quantity and quality. *Acta Crystallog. sect. D*, **55**, 1641-1653.
- Rubinson, K. A., Ladner, J. E., Tordova, M. & Gilliland, G. L. (2000). Cryosalts: suppression of ice formation in macromolecular crystallography. *Acta Crystallog. sect. D*, **56**, 996-1001.
- Samygina, V., Antonyuk, S., Lamzin, V. & Popov, A. (2000). Improving the X-ray resolution by reversible flash-cooling combined with concentration screening, as exemplified with PPase. *Acta Crystallog. sect. D*, **56**, 595-603.

31. Jacobson, R. H., Zhang, X. J., DuBose, R. F. & Matthews, B. W. (1994). Three-dimensional structure of β -galactosidase from *E. coli*. *Nature*, **369**, 761-766.
32. Juers, D. H., Jacobson, R. H., Wigley, D., Zhang, X.-J., Huber, R. E., Tronrud, D. E. & Matthews, B. W. (2000). High resolution refinement of β -galactosidase in a new crystal form reveals multiple metal-binding sites and provides a structural basis for α -complementation. *Protein Sci.* **9**, 1685-1699.
33. Matthews, B. W. (1968). Solvent content of protein crystals. *J. Mol. Biol.* **33**, 491-497.
34. Weik, M., Kryger, G., Schreurs, A. M. M., Bouma, B., Silman, I., Sussman, J. L. *et al.* (2001). Solvent behavior in flash-cooled protein crystals at cryogenic temperatures. *Acta Crystallog. sect. D*, **57**, 566-573.
35. Thomanek, U. F., Parak, F. & Mosbauer, R. L. (1973). Freezing of myoglobin crystals at high pressure. *Acta Crystallog. sect. A*, **29**, 263-265.
36. Ghormley, J. A. & Hochandel, C. J. (1971). Amorphous ice: density and reflectivity. *Science*, **171**, 62-64.
37. Mishima, O., Calvert, L. D. & Whalley, E. (1985). An apparently first-order transition between two amorphous phases of ice induced by pressure. *Nature*, **314**, 76-78.
38. Dubochet, J. & Lepault, J. (1984). Cryo-electron microscopy of vitrified water. *J. de Phys.* **45**, 85-94.
39. Juers, D. H. (2000). PhD Dissertation, p. 52, University of Oregon.
40. Ashcroft, N. & Mermin, D. (1976). *Solid State Physics*, Saunders College, Philadelphia.
41. Nemethy, G., Leach, S. J. & Scheraga, H. A. (1966). The influence of amino acid side chains on the free energy of helix-coil transitions. *J. Phys. Chem.* **70**, 998-1004.
42. Dasgupta, S., Iyer, G. H., Bryant, S. H., Lawrence, C. E. & Bell, J. A. (1997). Extent and nature of contacts between protein molecules in crystal lattices and between subunits of protein oligomers. *Proteins: Struct. Funct. Genet.* **28**, 494-514.
43. Zhang, X.-J. & Matthews, B. (1995). EDPDB: a multi-functional tool for protein structure analysis. *J. Appl. Crystallog.* **28**, 624-630.
44. Lee, B. & Richards, F. M. (1971). The interpretation of protein structures: estimation of static accessibility. *J. Mol. Biol.* **55**, 379-400.
45. Vriend, G. (1990). WHAT IF: a molecular modeling and drug design program. *J. Mol. Graph.* **8**, 52-56.
46. Dunbrack, R. L., Jr & Cohen, F. E. (1997). Bayesian statistical analysis of protein side-chain rotamer preferences. *Protein Sci.* **6**, 1661-1681.
47. Dewar, J. (1902). Coefficients of the cubical expansion of ice, hydrated salts, solid carbonic acid, and other substances at low temperatures. *Proc. Roy. Soc. London*, **70**, 237-247.
48. Connolly, M. L. (1983). Solvent-accessible surfaces of proteins and nucleic acids. *Science*, **221**, 709-713.
49. Kabsch, W. (1988). Evaluation of single X-ray diffraction data from a position sensitive detector. *J. Appl. Crystallog.* **21**, 916-924.
50. Leslie, A. (1990). *Crystallographic Computing*, Oxford University Press, Oxford.
51. Evans, P. R. (1993). Data reduction. In *Proceedings of a CCP4 Study Weekend on Data Collection and Processing*, pp. 114-122, Daresbury Laboratory, Warrington, UK.

Edited by P. E. Wright

(Received 8 March 2001; received in revised form 22 June 2001; accepted 28 June 2001)